

# Supplementary Information

## Self-organized amniogenesis by human pluripotent stem cells in a biomimetic implantation-like niche

Yue Shao<sup>1,†</sup>, Kenichiro Taniguchi<sup>2,†</sup>, Katherine Gurdziel<sup>3</sup>, Ryan F. Townshend<sup>2</sup>, Xufeng Xue<sup>1</sup>, Koh Meng Aw Yong<sup>1</sup>, Jianming Sang<sup>1</sup>, Jason R. Spence<sup>2</sup>, Deborah L. Gumucio<sup>2,\*</sup>, Jianping Fu<sup>1,2,4,\*</sup>

<sup>1</sup>Department of Mechanical Engineering, University of Michigan, Ann Arbor, MI 48109, USA;

<sup>2</sup>Department of Cell and Developmental Biology, University of Michigan Medical School, Ann Arbor,

MI 48109, USA; <sup>3</sup>Institute of Environmental Health Sciences, Wayne State University, Detroit, MI

48202, USA; <sup>4</sup>Department of Biomedical Engineering, University of Michigan, Ann Arbor, MI, 48109,

USA.

<sup>†</sup>These authors contributed equally to this work;

\*Correspondence should be addressed to J. F. (jpfu@umich.edu) or D. L. G.

(dgumucio@med.umich.edu).

This document contains:

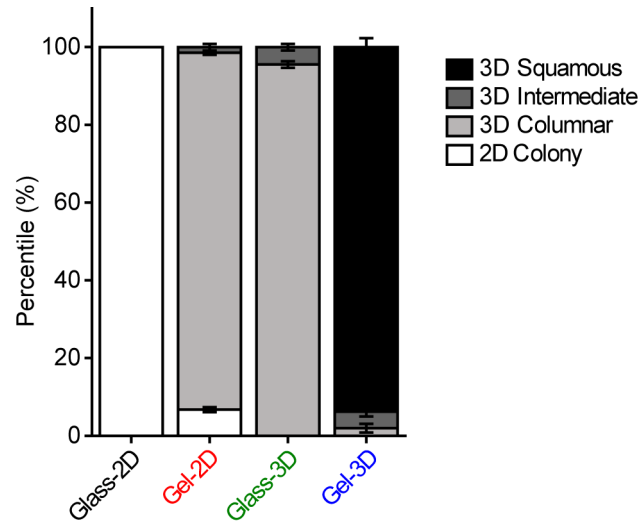
**Supplementary Figures and Captions**

**Supplementary Tables**

**Supplementary References**

## Supplementary Figures and Captions

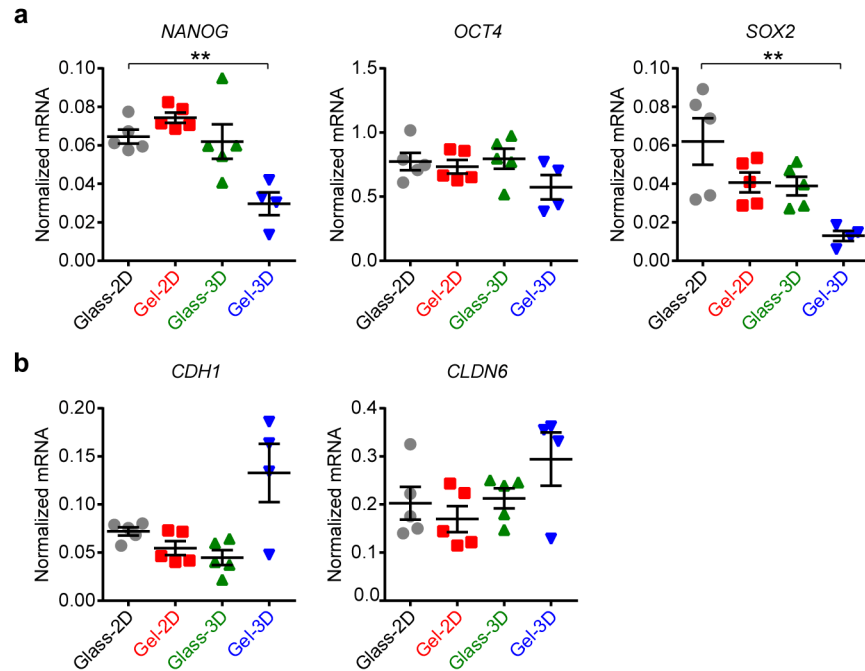
### Supplementary Figure 1



#### Supplementary Figure 1. Distinct morphogenesis of hPSCs under different culture conditions.

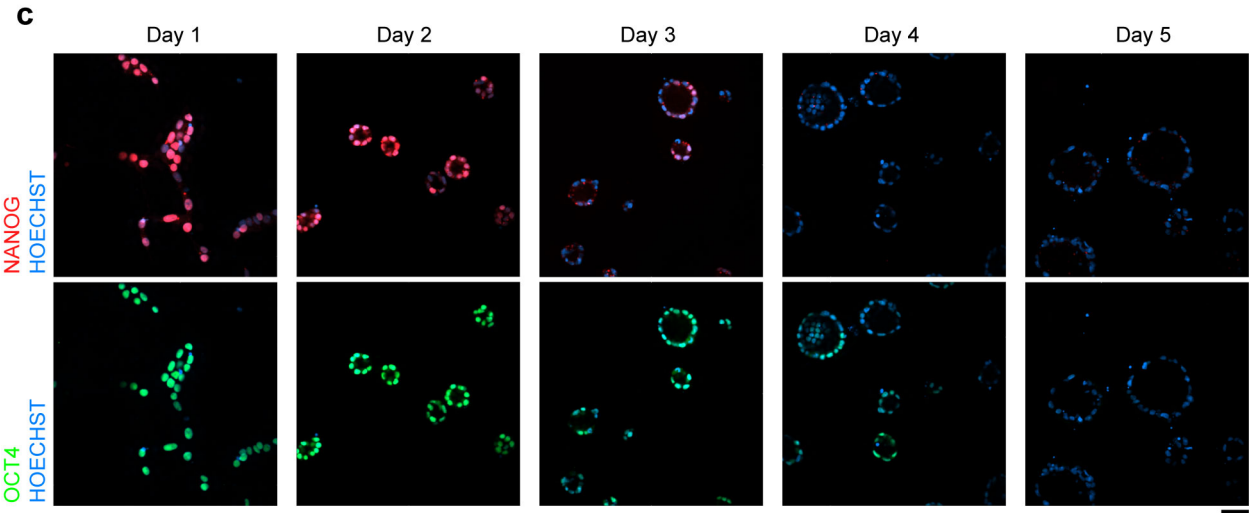
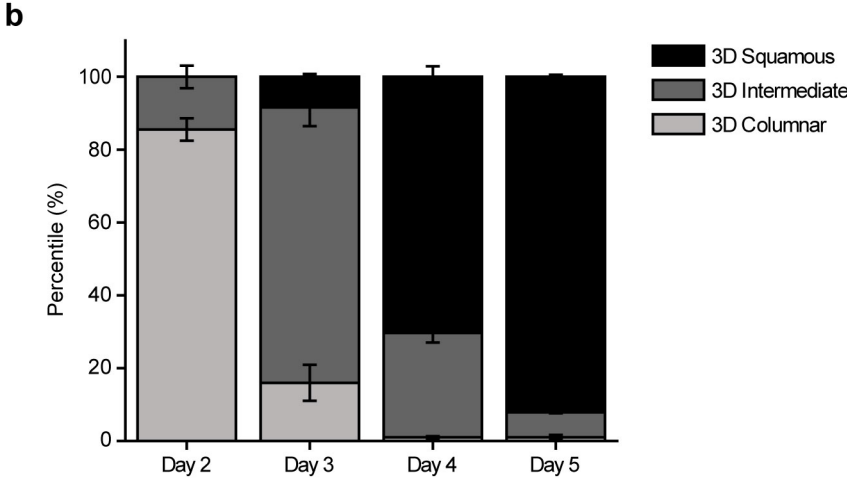
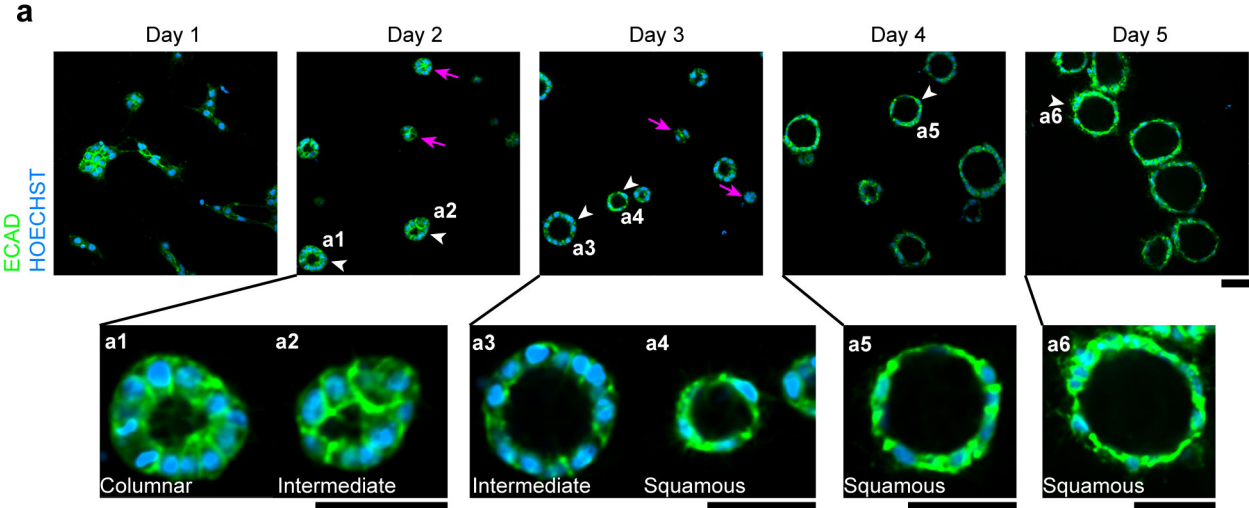
Stacked bar plots showing percentages of hPSC colonies or hPSC-derived epithelial cysts with different morphologies under different culture conditions as indicated. Semi-quantitative delineation of 3D columnar versus 3D squamous cysts was provided in **Fig. 1e**. A 3D intermediate cyst is defined as a cyst showing morphological transition from columnar to squamous (see also **Supplementary Fig. 3a**).  $n_{\text{cyst}}$  ( $n_{\text{colony}}$ ) = 100, 502, 469, and 694 for Glass-2D, Gel-2D, Glass-3D, and Gel-3D conditions, respectively. Data represent the mean  $\pm$  s.e.m with  $n = 3$  biological replicates from  $n = 2$  independent experiments. Same observation has been successfully repeated in total  $n = 16$  independent experiments.

## Supplementary Figure 2



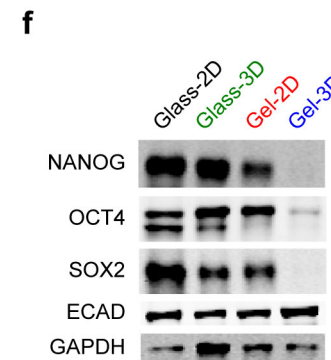
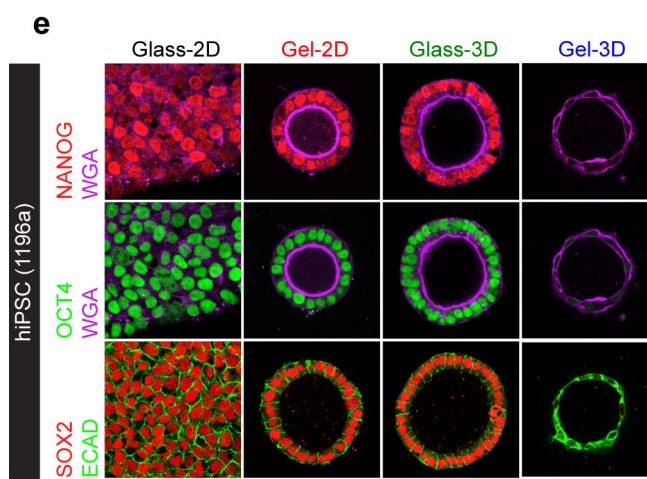
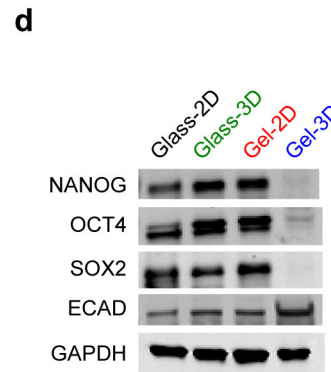
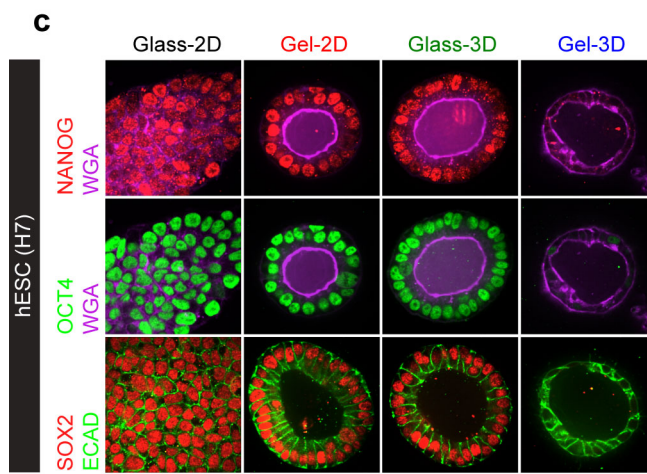
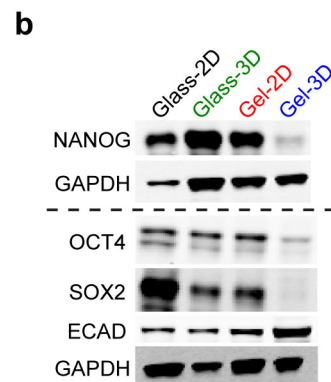
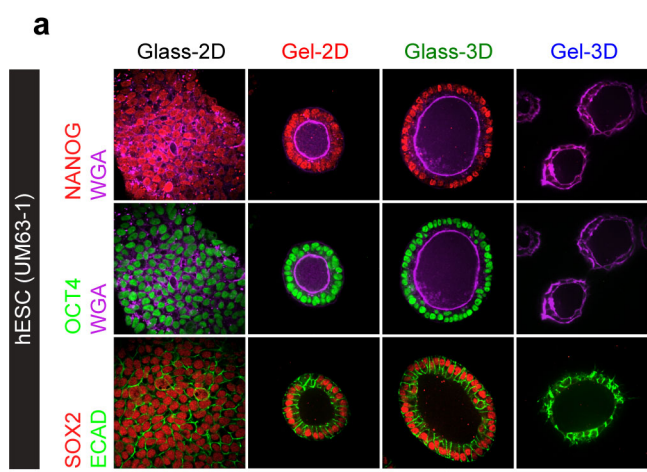
**Supplementary Figure 2. Squamous epithelial cysts derived from hPSCs show blunted transcriptional suppression of pluripotency genes while maintaining epithelial features.** qRT-PCR analysis of pluripotency genes *NANOG*, *OCT4*, and *SOX2* (a), as well as epithelial markers *CDH1* and *CLDN6* (b), for hPSCs cultured in indicated conditions. Data were normalized against *GAPDH* and plotted as the mean  $\pm$  s.e.m, with  $n = 4 - 5$  biological replicates indicated by individual dots under each condition.  $n = 2$  independent experiments.  $P$ -values were calculated using unpaired, two-sided Student's  $t$ -test. \*\*:  $P < 0.01$ .

**Supplementary Figure 3**



**Supplementary Figure 3. Morphogenic cytodifferentiation of hPSCs over time in the implantation-like Gel-3D niche.** (a) Confocal micrographs taken at different days (as indicated), showing immunostaining of ECAD (green) and counterstaining by HOECHST (blue) to examine morphological evolution of hPSCs cultured in the implantation-like Gel-3D niche. Magnified views of individual cysts (marked by white arrowheads) at different time points reveal a morphological transition from columnar to intermediate, to squamous cysts (**a1-a6**). Some hPSC clusters (marked by magenta arrows) did not form recognizable open lumens at day 2 or day 3. Such clusters were excluded from the quantification of time-dependent cyst morphological change in **b**. (b) Stacked bar plot showing percentages of hPSC-derived epithelial cysts with different morphologies in the implantation-like Gel-3D niche at days 2, 3, 4, and 5. Data represent the mean  $\pm$  s.e.m with  $n_{\text{cyst}} = 424$  (day 2), 534 (day 3), 652 (day 4), and 542 (day5).  $n = 3$  biological replicates for each condition. (c) Confocal micrographs showing co-staining of NANOG (red) and OCT4 (green) for hPSCs cultured in the implantation-like Gel-3D niche at different days as indicated. HOECHST (blue) counterstains the nucleus. Scale bars in **a&c**, 50  $\mu\text{m}$ .  $n = 2$  independent experiments.

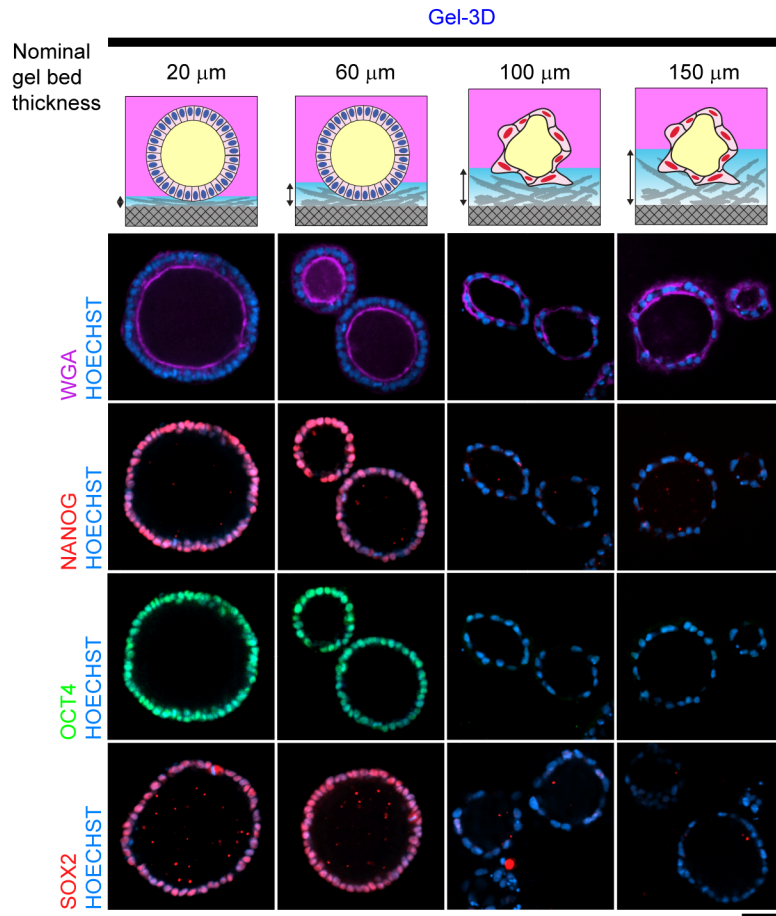
# Supplementary Figure 4



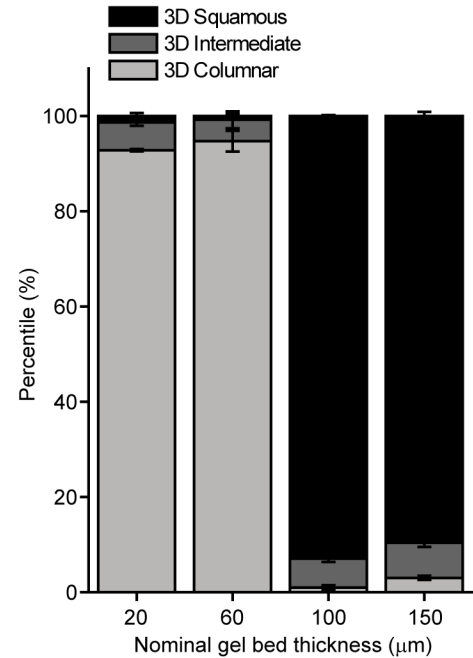
**Supplementary Figure 4. The implantation-like Gel-3D niche induces spontaneous, self-organized development of squamous epithelial cysts from multiple hPSC lines.** Confocal micrographs showing immunostaining of pluripotency markers NANOG (red; *top*), OCT4 (green; *middle*), and SOX2 (red; *bottom*), pan-cell membrane marker WGA (purple; *top and middle*), and basolateral membrane marker ECAD (green; *bottom*), in the UM63-1 hESC line (**a**), H7 hESC line (**c**), and 1196a hiPSC line (**e**) cultured under indicated conditions. Scale bars, 50  $\mu\text{m}$ . Western blot showing expression levels of NANOG, OCT4, SOX2, ECAD, and GAPDH in the UM63-1 hESC (**b**), H7 hESC (**d**), and 1196a hiPSC (**f**) cultured under indicated conditions. Immunofluorescence staining and Western blotting for each cell line was conducted for  $n = 2$  independent experiments.

## Supplementary Figure 5

**a**



**b**

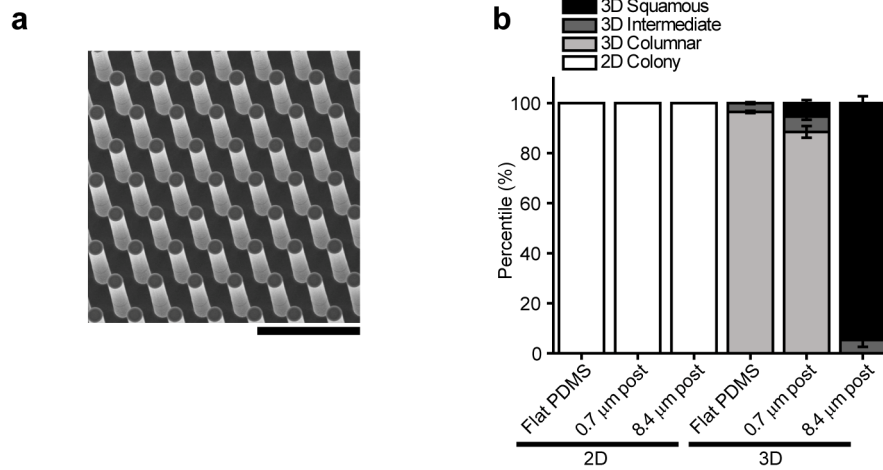


**Supplementary Figure 5. Self-organized development of squamous epithelial cystic tissues from hPSCs in the implantation-like Gel-3D niche requires a thick gel bed. (a)** Confocal micrographs showing immunostaining of WGA (purple), NANOG (red), OCT4 (green), and SOX2 (red) and counterstaining by HOECHST (blue) for hPSCs cultured in Gel-3D with varying nominal gel bed thicknesses as indicated. Cartoons show the typical epithelial cyst morphology observed under each condition.  $n = 2$  independent experiments. Scale bar, 50  $\mu\text{m}$ . **(b)** Stacked bar plot showing percentages of hPSC-derived epithelial cysts with different morphologies in Gel-3D as a function of the nominal gel bed thickness. Data represent the mean  $\pm$  s.e.m with  $n_{\text{cyst}} = 306, 361, 694,$  and 492 for gel beds of 20, 60,



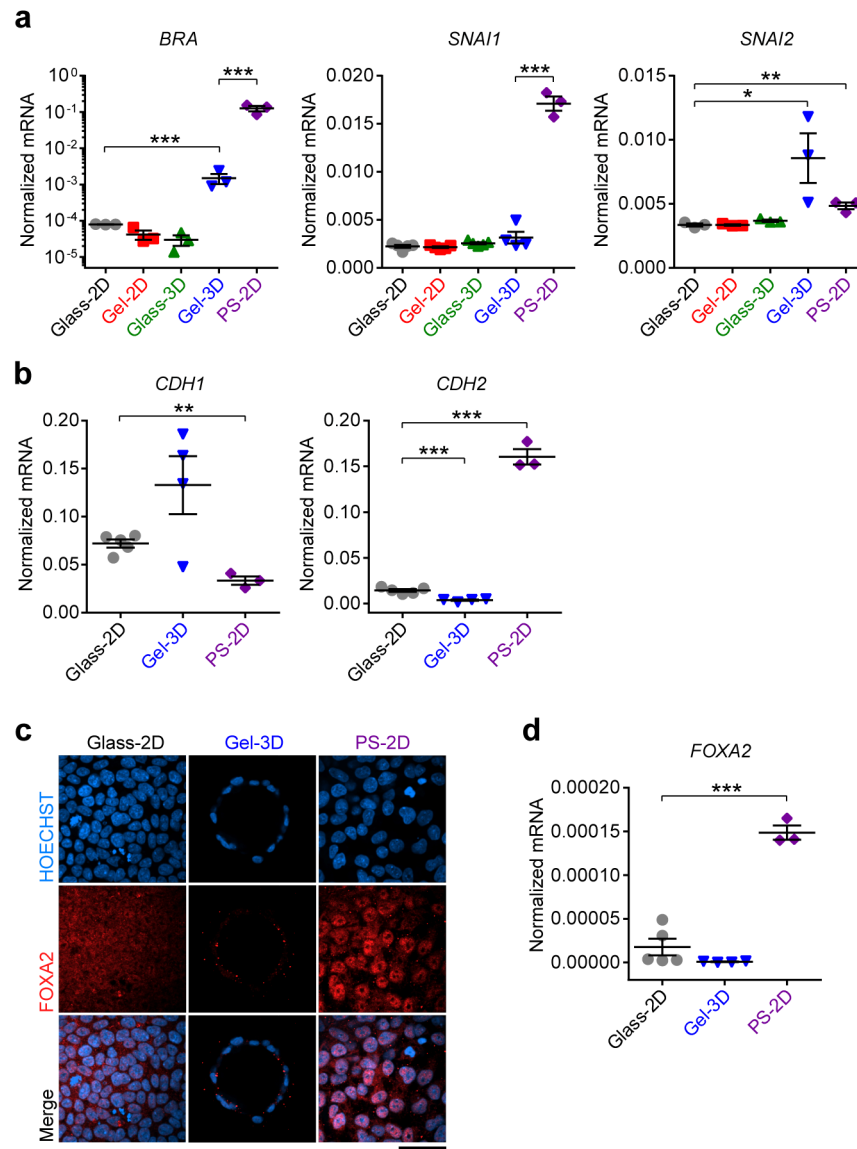
100, and 150  $\mu\text{m}$  thickness, respectively.  $n = 3$  biological replicates for each condition.  $n = 2$  independent experiments.

## Supplementary Figure 6



**Supplementary Figure 6. An artificial matrix containing an elastomeric micropost array supports self-organized development of hPSCs into epithelial cystic tissues with squamous, human amnion-like morphology. (a)** Scanning electron microscopy (SEM) image of the elastomeric polydimethylsiloxane (PDMS) micropost array with a post diameter of  $1.83 \mu\text{m}$ , a post height of  $8.4 \mu\text{m}$ , and a post center-to-center distance of  $4 \mu\text{m}$ . Scale bar,  $10 \mu\text{m}$ . **(b)** Stacked bar plot showing percentages of hPSC colony or hPSC-derived epithelial cysts with different morphologies as a function of PDMS micropost height and ECM dimensionality. Flat PDMS surfaces without microposts (thus with a micropost height of  $0 \mu\text{m}$ ) were included for comparison. Data represent the mean  $\pm$  s.e.m with  $n_{\text{colony}} = 100$  for all three 2D culture conditions and  $n_{\text{cyst}} = 250, 270,$  and  $282$  for 3D cultures using flat PDMS,  $0.7 \mu\text{m}$  tall micropost, and  $8.4 \mu\text{m}$  tall micropost, respectively.  $n = 3$  biological replicates for each condition.  $n = 3$  independent experiments.

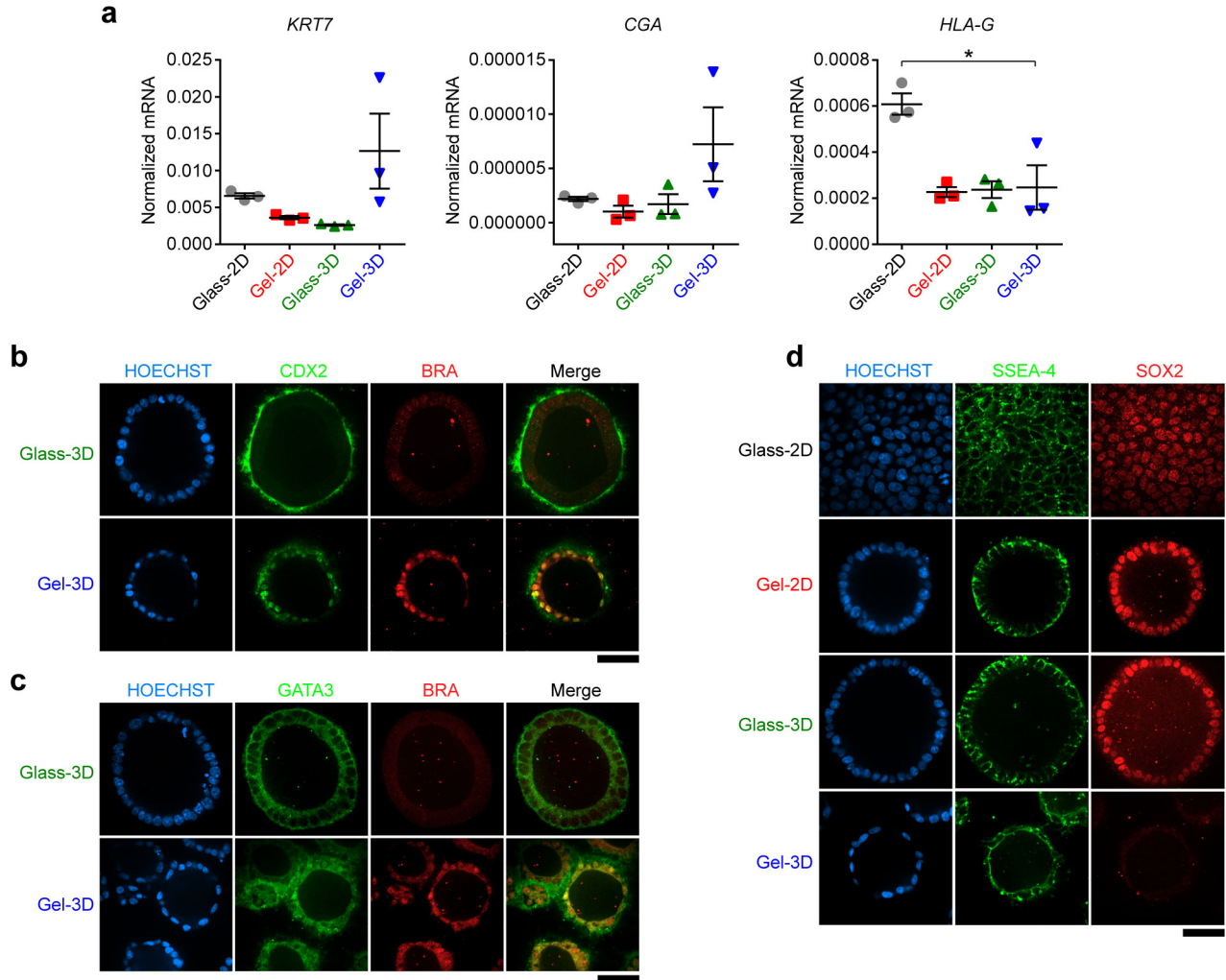
## Supplementary Figure 7



**Supplementary Figure 7. Development of squamous cystic tissues by hPSCs in the implantation-like Gel-3D niche activates a unique subset of epithelial-to-mesenchymal transition-related transcription factors. (a,b)** qRT-PCR analysis of *BRACHYURY* (*BRA*), *SNAIL*, *SNAI2* (a), *CDH1*, and *CDH2* (b), for hPSCs cultured in indicated conditions. Data were normalized against *GAPDH* and plotted as the mean  $\pm$  s.e.m, with  $n = 3 - 5$  biological replicates indicated by individual dots under each condition,  $n = 2$  independent experiments. Data in b for *CDH1* under both Glass-2D and Gel-3D conditions are the same as those in **Supplementary Fig. 2b**. (c) Confocal

micrographs showing immunostaining of FOXA2 (red) and counterstaining by HOECHST (blue) for hPSCs cultured in Glass-2D, Gel-3D, and PS-2D conditions as indicated. Scale bar, 50  $\mu\text{m}$ .  $n = 2$  independent experiments. **(d)** qRT-PCR analysis of *FOXA2* for hPSCs cultured in different conditions as indicated. Data were normalized against *GAPDH* and plotted as the mean  $\pm$  s.e.m, with  $n = 3 - 5$  biological replicates indicated by individual dots under each condition. *P*-values were calculated using unpaired, two-sided Student's *t*-test. \*:  $P < 0.05$ ; \*\*:  $P < 0.01$ ; \*\*\*:  $P < 0.001$ .  $n = 2$  independent experiments.

## Supplementary Figure 8



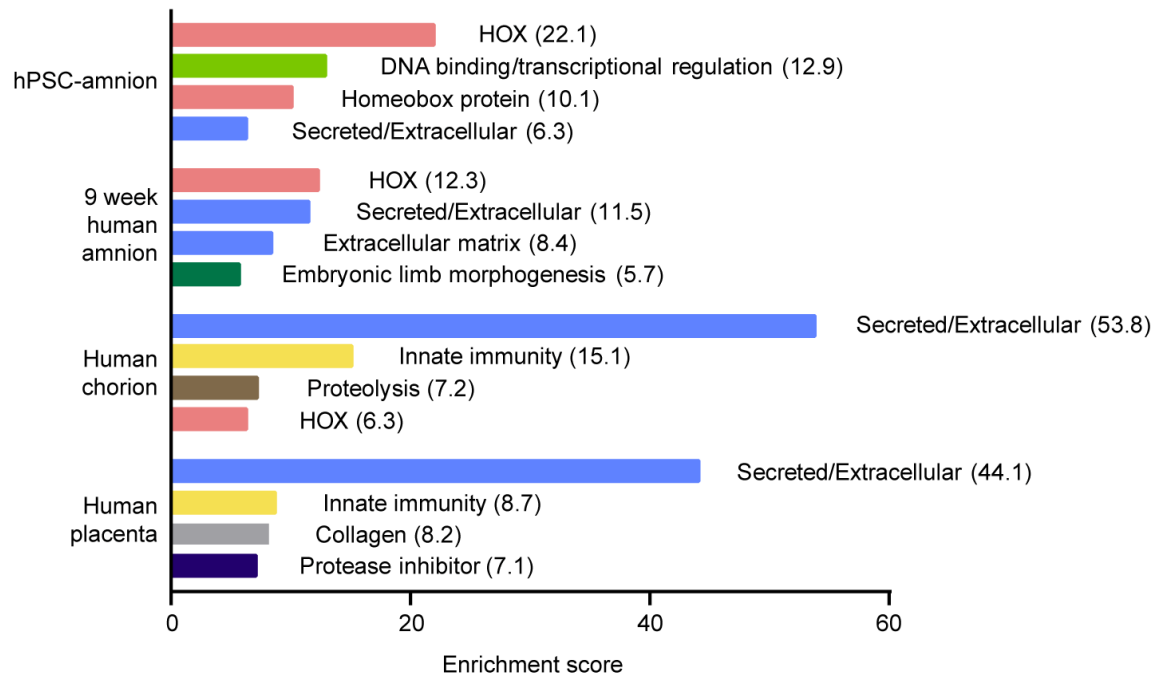
### Supplementary Figure 8. hPSC-derived squamous cystic tissue lacks molecular features

**associated with trophoblasts.** (a) qRT-PCR analysis of trophoblast markers *KRT7*, *CGA*, and *HLA-G*, for hPSCs under different culture conditions as indicated. Data were normalized against *GAPDH* before being plotted as the mean  $\pm$  s.e.m, with  $n = 3$  biological replicates indicated by individual dots for each condition.  $n = 2$  independent experiments.  $P$ -values were calculated using unpaired, two-sided Student's  $t$ -test. \*:  $P < 0.05$ . (b&c) Confocal micrographs showing co-staining of BRA (red) with CDX2 (green; b) or GATA3 (green; c), for hPSCs under both Glass-3D and Gel-3D culture conditions. HOECHST (blue) counterstains the nucleus.  $n = 2$  independent experiments. (d) Confocal micrographs showing co-

staining of SSEA-4 (green) with SOX2 (red) for hPSCs cultured in different conditions as indicated.

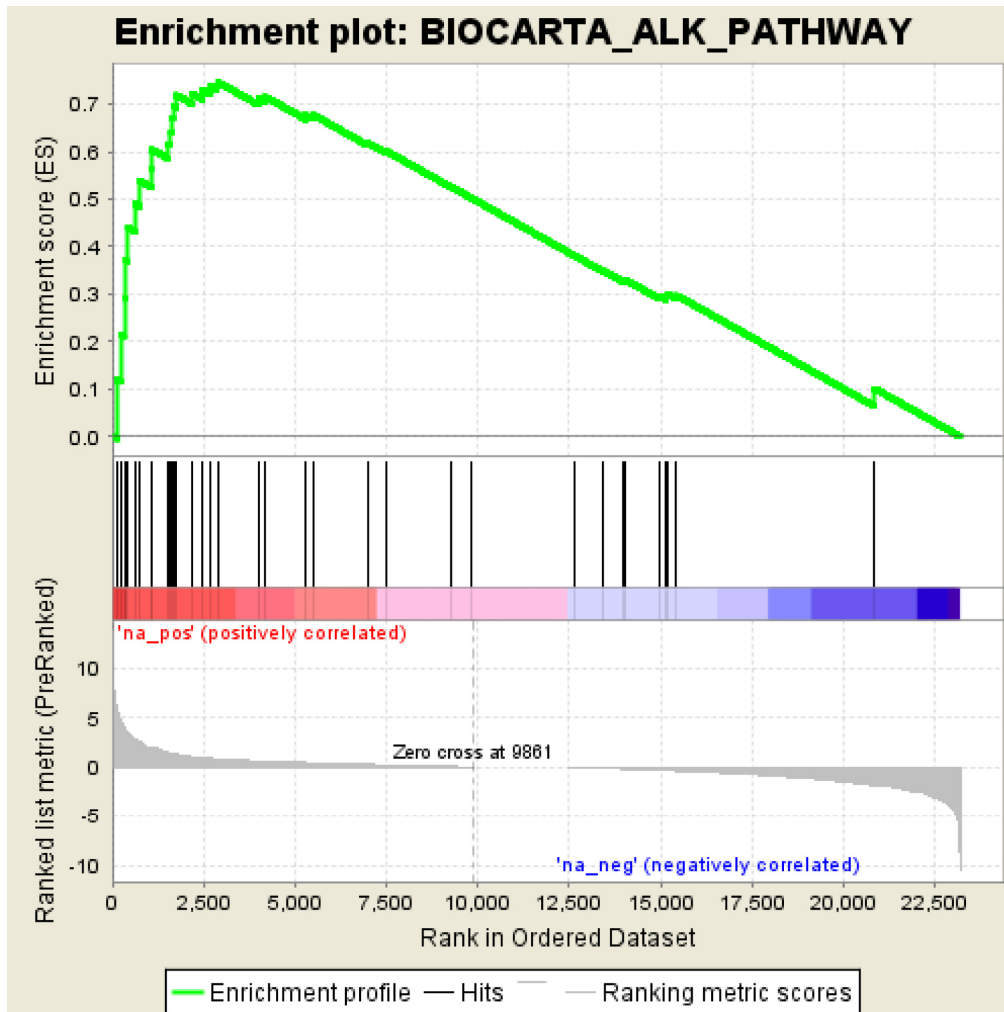
HOECHST (blue) counterstains the nucleus.  $n = 2$  independent experiments. Scale bars in **b-d**, 50  $\mu\text{m}$ .

## Supplementary Figure 9



**Supplementary Figure 9. Gene ontology (GO) functional annotation clustering.** Genes enriched in hPSC-amnion, 9-week human amnion, human chorion, and human placenta, respectively, relative to hPSCs, were subjected to functional annotation clustering analysis using DAVID. For each data set, the four annotation clusters with the highest enrichment scores (plotted along the *x*-axis and also listed in parentheses following the annotation term) are presented. The data sets used for 9-week human amnion, human chorion, and human placenta are from a previous publication (GEO accession number GSE66302)<sup>1</sup>.

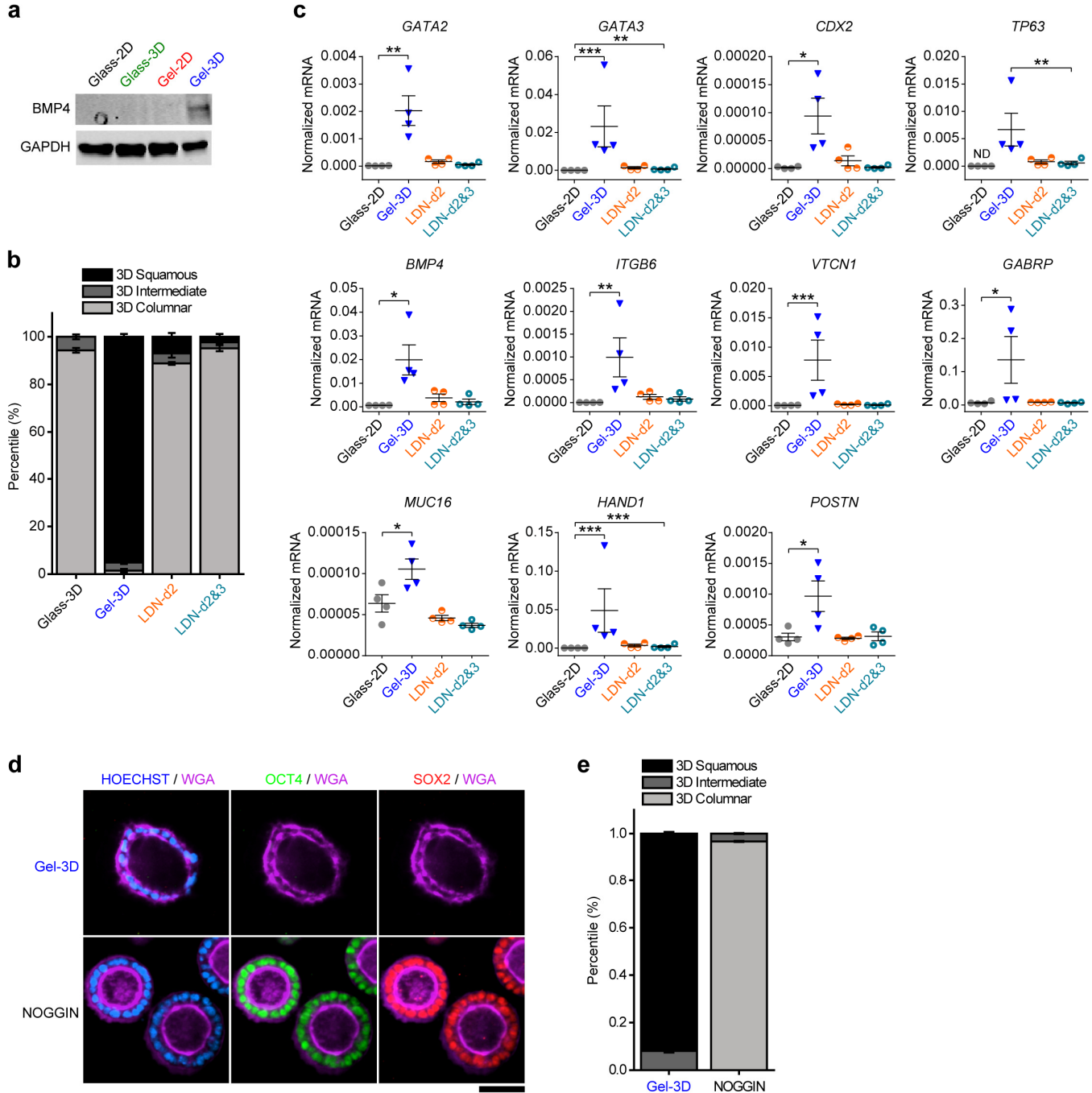
### Supplementary Figure 10



**Supplementary Figure 10. Gene set enrichment analysis (GSEA) for 35 ALK-pathway genes in hPSC-amnion.** The entire ranked list of genes, ordered by fold change of expression level in hPSC-amnion relative to hPSCs (as shown in **Supplementary Table 1**), was queried using the gene set, BIOCARTA\_ALK\_PATHWAY, which contains 35 genes associated with BMP signaling. Significant enrichment of ALK-pathway related genes was observed in hPSC-amnion. (see **Supplementary Table 5** for tabulated enrichment analysis results).



## Supplementary Figure 11



**Supplementary Figure 11. BMP signaling is required for the development of amnion-like squamous tissue from hPSCs.** (a) Western blot showing expression levels of BMP4 and GAPDH in cells cultured under different conditions as indicated. (b) Stacked bar plot showing percentages of hPSC-derived epithelial cysts with different morphologies in Glass-3D supplemented with DMSO

(Glass-3D; negative control), in Gel-3D supplemented with DMSO (Gel-3D; positive control), and in Gel-3D supplemented with LDN193189 (LDN; 500 nM) on day 2 only (LDN-d2) or on both days 2 and 3 (LDN-d2&3).  $n_{\text{cyst}} = 144, 311, 365, \text{ and } 320$  for Glass-3D, Gel-3D, LDN-d2, and LDN-d2&3, respectively.  $n = 3$  biological replicates for each condition.  $n = 2$  independent experiments. **(c)** qRT-PCR analysis of *GATA2*, *GATA3*, *CDX2*, *TP63*, *BMP4*, *ITGB6*, *VTCN1*, *GABRP*, *MUC16*, *HAND1*, and *POSTN* under Glass-3D, Gel-3D, LDN-d2, and LDN-d2&3 conditions. Data were normalized against *GAPDH* and plotted as the mean  $\pm$  s.e.m, with  $n = 4$  biological replicates indicated by individual dots for each condition.  $n = 2$  independent experiments. *ND*, not detected, with its normalized value set to zero. *P*-values were calculated using unpaired, two-sided Student's *t*-test. *P*-value calculation was not performed against "*ND*" result. \*:  $P < 0.05$ ; \*\*:  $P < 0.01$ ; \*\*\*:  $P < 0.001$ . **(d)** Immunofluorescence analysis of cysts cultured under Gel-3D condition without (top panel) or with (bottom panel) NOGGIN treatment. Cysts were stained for OCT4 (green), SOX2 (red), and WGA (purple). HOECHST (blue) counterstains the nucleus. Scale bar, 50  $\mu\text{m}$ . **(e)** Stacked bar plots show percentages of hPSC-derived epithelial cysts with different morphologies in the Gel-3D system without ("Gel-3D" group) or with ("NOGGIN" group) NOGGIN treatment.  $n_{\text{cyst}} = 131$  and 241 for Gel-3D and NOGGIN groups, respectively. Data represent the mean  $\pm$  s.e.m. with  $n = 3$  biological replicates from  $n = 2$  independent experiments.

## **Supplementary Tables**

**Supplementary Table 1. Processed RNA-seq reads for control hPSCs (Glass-2D) and hPSC-  
amnion (Gel-3D).**

**(see separate Supplementary File)**

**Supplementary Table 2. List of 108 putative pluripotency genes<sup>2</sup> detected in hPSCs and hPSC-  
 amnion in RNA-seq. Genes are consecutively listed as plotted, from left to right, in Fig. 4f.**

<b>1</b>	<i>CUZD1</i>	<b>28</b>	<i>SCLY</i>	<b>55</b>	<i>TOMM40</i>	<b>82</b>	<i>RLIM</i>
<b>2</b>	<i>CER1</i>	<b>29</b>	<i>TXLNG</i>	<b>56</b>	<i>SEPHS1</i>	<b>83</b>	<i>RC3H2</i>
<b>3</b>	<i>CCL26</i>	<b>30</b>	<i>JMJD1C</i>	<b>57</b>	<i>SLIRP</i>	<b>84</b>	<i>PINX1</i>
<b>4</b>	<i>LEFTY2</i>	<b>31</b>	<i>EIF2AK4</i>	<b>58</b>	<i>EMG1</i>	<b>85</b>	<i>RPRM</i>
<b>5</b>	<i>GDF3</i>	<b>32</b>	<i>TARS</i>	<b>59</b>	<i>DDX18</i>	<b>86</b>	<i>GRPR</i>
<b>6</b>	<i>ADD2</i>	<b>33</b>	<i>SNURF</i>	<b>60</b>	<i>MTAP</i>	<b>87</b>	<i>GNPTAB</i>
<b>7</b>	<i>DDX21</i>	<b>34</b>	<i>RRP15</i>	<b>61</b>	<i>TFAM</i>	<b>88</b>	<i>FGF2</i>
<b>8</b>	<i>PNO1</i>	<b>35</b>	<i>USP45</i>	<b>62</b>	<i>NIP7</i>	<b>89</b>	<i>MYO1E</i>
<b>9</b>	<i>DPPA4</i>	<b>36</b>	<i>SHISA9</i>	<b>63</b>	<i>HSPD1</i>	<b>90</b>	<i>LARP7</i>
<b>10</b>	<i>RRAS2</i>	<b>37</b>	<i>NANOG</i>	<b>64</b>	<i>TIMM8A</i>	<b>91</b>	<i>CACHD1</i>
<b>11</b>	<i>GABRB3</i>	<b>38</b>	<i>CCRN4L</i>	<b>65</b>	<i>POU5F1</i>	<b>92</b>	<i>PHC1</i>
<b>12</b>	<i>RPL22L1</i>	<b>39</b>	<i>C10orf76</i>	<b>66</b>	<i>POU5F1P3</i>	<b>93</b>	<i>VRTN</i>
<b>13</b>	<i>MDN1</i>	<b>40</b>	<i>EXOC2</i>	<b>67</b>	<i>DDX6</i>	<b>94</b>	<i>TERF1</i>
<b>14</b>	<i>GAL</i>	<b>41</b>	<i>G3BP2</i>	<b>68</b>	<i>CENPN</i>	<b>95</b>	<i>CHAC2</i>
<b>15</b>	<i>PMAIP1</i>	<b>42</b>	<i>PHAX</i>	<b>69</b>	<i>TUBB2B</i>	<b>96</b>	<i>TDGF1</i>
<b>16</b>	<i>BICD1</i>	<b>43</b>	<i>CDC25A</i>	<b>70</b>	<i>DENR</i>	<b>97</b>	<i>SLC25A21</i>
<b>17</b>	<i>AKIRIN1</i>	<b>44</b>	<i>MTHFD1L</i>	<b>71</b>	<i>CASP3</i>	<b>98</b>	<i>USP44</i>
<b>18</b>	<i>FGD6</i>	<b>45</b>	<i>RNASEH1</i>	<b>72</b>	<i>SKP2</i>	<b>99</b>	<i>LEFTY1</i>
<b>19</b>	<i>MRS2</i>	<b>46</b>	<i>LITD1</i>	<b>73</b>	<i>MKKS</i>	<b>100</b>	<i>NODAL</i>
<b>20</b>	<i>BPTF</i>	<b>47</b>	<i>LRR1</i>	<b>74</b>	<i>NUDT15</i>	<b>101</b>	<i>RRM2</i>
<b>21</b>	<i>KIF13A</i>	<b>48</b>	<i>MRPS30</i>	<b>75</b>	<i>FKBP4</i>	<b>102</b>	<i>GLB1L3</i>
<b>22</b>	<i>RAC3</i>	<b>49</b>	<i>PSME3</i>	<b>76</b>	<i>NUP160</i>	<b>103</b>	<i>C21orf88</i>
<b>23</b>	<i>C9orf85</i>	<b>50</b>	<i>MSH2</i>	<b>77</b>	<i>TMPO</i>	<b>104</b>	<i>SMPDL3B</i>
<b>24</b>	<i>DNAH14</i>	<b>51</b>	<i>EEF1E1</i>	<b>78</b>	<i>MMS22L</i>	<b>105</b>	<i>UNC5D</i>
<b>25</b>	<i>METTL21A</i>	<b>52</b>	<i>NLN</i>	<b>79</b>	<i>ESRP1</i>	<b>106</b>	<i>LECT1</i>
<b>26</b>	<i>METTL8</i>	<b>53</b>	<i>LOC100506054</i>	<b>80</b>	<i>SKIL</i>	<b>107</b>	<i>ZIC3</i>
<b>27</b>	<i>BCAT1</i>	<b>54</b>	<i>NOLC1</i>	<b>81</b>	<i>SNX5</i>	<b>108</b>	<i>RTP1</i>

**Supplementary Table 3. List of 50 most up-regulated genes (UP-50) and 50 most down-regulated genes (DOWN-50) in hPSC-amnion compared with hPSCs. Genes are consecutively listed as plotted, from left to right, in Fig. 4f.**

UP-50 genes				DOWN-50 genes			
Rank	Gene	Rank	Gene	Rank	Gene	Rank	Gene
1	<i>HAND1</i>	26	<i>PLSCR5</i>	1	<i>CUZD1</i>	26	<i>VTN</i>
2	<i>TFAP2B</i>	27	<i>HOXC13</i>	2	<i>CH25H</i>	27	<i>IFITM5</i>
3	<i>ISL1</i>	28	<i>MEIS1</i>	3	<i>PTGFR</i>	28	<i>MIRLET7BHG</i>
4	<i>LUM</i>	29	<i>WNT6</i>	4	<i>TMPRSS3</i>	29	<i>LOC399829</i>
5	<i>C8orf4</i>	30	<i>NR2F2</i>	5	<i>JAKMIP2-AS1</i>	30	<i>XIST</i>
6	<i>EVX1</i>	31	<i>MSX2</i>	6	<i>ANKRD22</i>	31	<i>KCNJ1</i>
7	<i>DLX5</i>	32	<i>CCR1</i>	7	<i>ISL2</i>	32	<i>UCP1</i>
8	<i>TBX3</i>	33	<i>CYSLTR2</i>	8	<i>RXFP1</i>	33	<i>TNFAIP6</i>
9	<i>HOXB2</i>	34	<i>EPAS1</i>	9	<i>PCDHB1</i>	34	<i>C3orf72</i>
10	<i>ERP27</i>	35	<i>KRT23</i>	10	<i>OLIG3</i>	35	<i>SEZ6</i>
11	<i>COL3A1</i>	36	<i>TP63</i>	11	<i>WDR49</i>	36	<i>CBLN4</i>
12	<i>GATA3</i>	37	<i>MEIS1-AS3</i>	12	<i>AQP7</i>	37	<i>LOC100127888</i>
13	<i>GUCY1A3</i>	38	<i>BARX2</i>	13	<i>NLRP10</i>	38	<i>FREM3</i>
14	<i>P2RY6</i>	39	<i>HMX1</i>	14	<i>NPTX1</i>	39	<i>TMEM114</i>
15	<i>TNFSF8</i>	40	<i>HOXC6</i>	15	<i>LOC100507387</i>	40	<i>DRD1</i>
16	<i>TFAP2A</i>	41	<i>HOXB-AS1</i>	16	<i>TAC1</i>	41	<i>DSG3</i>
17	<i>DCN</i>	42	<i>IGFBP7</i>	17	<i>GABRA1</i>	42	<i>PRSS56</i>
18	<i>VGLL1</i>	43	<i>DIO3</i>	18	<i>FOXE1</i>	43	<i>CCR9</i>
19	<i>HOXB9</i>	44	<i>HOXB3</i>	19	<i>NXF4</i>	44	<i>GPR17</i>
20	<i>GATA3-AS1</i>	45	<i>LOC642366</i>	20	<i>TPH2</i>	45	<i>PAPLN</i>
21	<i>CDX2</i>	46	<i>ITGA8</i>	21	<i>RUFY4</i>	46	<i>COL20A1</i>
22	<i>PGLYRP4</i>	47	<i>C1orf105</i>	22	<i>HTR1A</i>	47	<i>HMX2</i>
23	<i>SLC40A1</i>	48	<i>ANKRD1</i>	23	<i>SERPINB4</i>	48	<i>LOC100507244</i>
24	<i>CHI3L2</i>	49	<i>LCPI</i>	24	<i>NEUROG3</i>	49	<i>TPSB2</i>
25	<i>HAND2</i>	50	<i>DLX6</i>	25	<i>CDH19</i>	50	<i>MPO</i>

**Supplementary Table 4. List of hierarchically clustered ~4,000 pre-selected genes that have greater expression in hPSC-amnion than in hPSCs and in fetal extraembryonic tissues<sup>1</sup>. Genes are consecutively listed as plotted, from top to bottom, in Fig. 4g.**

**(See separate Supplementary File)**

**Supplementary Table 5. Tabulated gene set enrichment analysis (GSEA) results. The entire data set (hPSC-amnion versus hPSCs), as ranked and shown in Supplementary Table 1, was queried using the gene set, BIOCARTA\_ALK\_PATHWAY, a collection of 35 genes related to BMP signaling.**

<b>Data set</b>		<b>Supplementary Table 1</b>				
<b>Gene set</b>		<b>BIOCARTA_ALK_PATHWAY</b>				
<b>Enrichment score (ES)</b>		0.7473358				
<b>Normalized enrichment score (NES)</b>		2.1402795				
<b>Nominal p-value</b>		0				
<b>FDR q-value</b>		0				
<b>FWER p-value</b>		0				
	PROBE	GENE SYMBOL	RANK IN GENE LIST	RANK METRIC SCORE	RUNNING ES	CORE ENRICHMENT
1	BMP4	BMP4	123	6.028	0.1195	Yes
2	NOG	NOG	224	4.789	0.2144	Yes
3	TGFB2	TGFB2	328	3.962	0.2919	Yes
4	SMAD6	SMAD6	348	3.879	0.3714	Yes
5	BMP5	BMP5	434	3.509	0.4404	Yes
6	FZD1	FZD1	618	2.794	0.4904	Yes
7	NKX2-5	NKX2-5	754	2.632	0.5391	Yes
8	NPPB	NPPB	1070	1.929	0.5654	Yes
9	BMP10	BMP10	1088	1.924	0.6045	Yes
10	BMP2	BMP2	1517	1.479	0.6166	Yes
11	NPPA	NPPA	1598	1.408	0.6424	Yes
12	TGFB1	TGFB1	1638	1.381	0.6693	Yes
13	GATA4	GATA4	1660	1.356	0.6964	Yes
14	CHRD	CHRD	1747	1.294	0.7195	Yes
15	BMPR2	BMPR2	2175	1.04	0.7226	Yes
16	BMP7	BMP7	2468	0.935	0.7294	Yes
17	GSK3B	GSK3B	2661	0.885	0.7394	Yes
18	CTNNB1	CTNNB1	2873	0.824	0.7473	Yes
19	SMAD1	SMAD1	4004	0.62	0.7114	No
20	BMPR1A	BMPR1A	4196	0.593	0.7154	No
21	SMAD5	SMAD5	5296	0.452	0.6773	No
22	MEF2C	MEF2C	5496	0.428	0.6776	No
23	MAP3K7	MAP3K7	6985	0.268	0.6188	No
24	HNF1A		7505	0.217	0.6009	No
25	ATF2	ATF2	9280	0.063	0.5256	No
26	SMAD4	SMAD4	9814	0.005	0.5027	No
27	RFC1	RFC1	12640	-0.02	0.3811	No
28	ACVR1	ACVR1	13433	-0.105	0.349	No
29	TGFBR2	TGFBR2	13945	-0.164	0.3304	No
30	AXIN1	AXIN1	14035	-0.175	0.3301	No
31	DVL1	DVL1	14975	-0.301	0.2958	No

32	TGFB3	TGFB3	15146	-0.327	0.2953	No
33	APC	APC	15186	-0.333	0.3005	No
34	TGFBR1	TGFBR1	15434	-0.371	0.2975	No
35	MYL2	MYL2	20846	-1.802	0.1011	No
35	MYL2	MYL2	20846	-1.802	0.1011	No



**Supplementary Table 6. List of primary antibodies used in immunocytochemistry (ICC) and Western blotting (WB).**

Protein	Species	Application	Catalog No.	Vendor
EZRIN	Mouse	1:2000 (ICC)	E8897	Sigma-Aldrich
E-CADHERIN	Mouse	1:500 (ICC) 1:1000 (WB)	610181	BD Biosciences
NANOG	Rabbit	1:500 (ICC) 1:2000 (WB)	4903S	Cell Signaling Technology
OCT4	Mouse	1:200 (ICC) 1:500 (WB)	SC-5279	Santa-Cruz Biotechnology
SOX2	Rabbit	1:1000 (ICC) 1:1000 (WB)	09-0024	Stemgent
GAPDH	Rabbit	1:1000 (WB)	SC-25778	Santa-Cruz Biotechnology
BRACHYURY	Rabbit	1:100 (ICC)	SC-20109	Santa-Cruz Biotechnology
SNAIL	Rabbit	1:100 (ICC)	SC-28199	Santa-Cruz Biotechnology
SLUG	Rabbit	1:400 (ICC)	9585	Cell Signaling Technology
N-CADHERIN	Rat	1:500 (ICC)	MNCD2-c	Developmental Studies Hybridoma Bank
FOXA2	Rabbit	1:500 (ICC)	WRAB-1200	Seven Hills Bioreagents
pSMAD1/5	Rabbit	1:100 (ICC) 1:1000 (WB)	9516S	Cell Signaling Technology
SMAD1/5/8	Rabbit	1:1000 (WB)	SC-6031-R	Santa-Cruz Biotechnology
CDX2	Mouse	1:500 (ICC)	MU392A-5UC	Biogenex
GATA3	Mouse	1:100 (ICC)	SC-268	Santa-Cruz Biotechnology
SSEA-4	Mouse	1:500 (ICC)	MAB4304	EMD Millipore
BMP4	Mouse	1:1000 (WB)	4680	Cell Signaling Technology

**Supplementary Table 7. List of qRT-PCR primers.**

Gene	Primer Sequences (5' -> 3')	Reference
<i>NANOG</i>	Forward: GATTTGTGGGCCTGAAGAAA	NA
	Reverse: ATGGAGGAGGGAAGAGGAGA	NA
<i>OCT4</i>	Forward: GTGGAGGAAGCTGACAACAA	NA
	Reverse: GGTTCTCGATACTGGTTTCGC	NA
<i>SOX2</i>	Forward: GCTTAGCCTCGTCGATGAAC	NA
	Reverse: AACCCCAAGATGCACAACCTC	NA
<i>GAPDH</i>	Forward: CTCTGCTCCTCCTGTTTCGAC	NA
	Reverse: TTAAAAGCAGCCCTGGTGAC	NA
<i>CDH1</i>	Forward: TCTTCAATCCCACCACGTACA	NA
	Reverse: TGCCATCGTTGTTCACTGGA	NA
<i>CDH2</i>	Forward: ATCAACCCCATACACCAGCC	NA
	Reverse: GTCGATTGGTTTGACCACGG	NA
<i>CLDN6</i>	Forward: TGTTCCGGCTTGCTGGTCTAC	PrimerBank <sup>3</sup>
	Reverse: CGGGGATTAGCGTCAGGAC	PrimerBank
<i>BRACHYURY</i>	Forward: TGCTGCAATCCCATGACA	PrimerBank
	Reverse: CGTTGCTCACAGACCACA	PrimerBank
<i>SNAI1</i>	Forward: TCGGAAGCCTAACTACAGCGA	PrimerBank
	Reverse: AGATGAGCATTGGCAGCGAG	PrimerBank
<i>SNAI2</i>	Forward: CGAACTGGACACACATACAGTG	PrimerBank
	Reverse: CTGAGGATCTCTGGTTGTGGT	PrimerBank
<i>FOXA2</i>	Forward: CGACTGGAGCAGCTACTATGC	NA
	Reverse: TACGTGTTTCATGCCGTTTCAT	NA
<i>GATA2</i>	Forward: CAGCAAGGCTCGTTCCTGTT	PrimerBank
	Reverse: GGCTTGATGAGTGGTTCGGT	PrimerBank
<i>GATA3</i>	Forward: GCCCCTCATTAAGCCCAAG	PrimerBank
	Reverse: TTGTGGTGGTCTGACAGTTCG	PrimerBank
<i>CDX2</i>	Forward: GACGTGAGCATGTACCCTAGC	PrimerBank
	Reverse: GCGTAGCCATTCCAGTCCT	PrimerBank
<i>TP63</i>	Forward: CTGGAAAACAATGCCCAGA	Li et al. <sup>4</sup>
	Reverse: AGAGAGCATCGAAGGTGGAG	Li et al. <sup>4</sup>
<i>GATA4</i>	Forward: CGACACCCCAATCTCGATATG	PrimerBank
	Reverse: GTTGCACAGATAGTGACCCGT	PrimerBank
<i>GATA6</i>	Forward: CTCAGTTCCTACGCTTCGCAT	PrimerBank
	Reverse: GTCGAGGTCAGTGAACAGCA	PrimerBank
<i>KRT7</i>	Forward: AGGATGTGGATGCTGCCTAC	Li et al. <sup>4</sup>

	<i>Reverse:</i> CACCACAGATGTGTCGGAGA	Li <i>et al.</i> <sup>4</sup>
<i>CGA</i>	<i>Forward:</i> CACTCCACTAAGGTCCAAGAAGA	PrimerBank
	<i>Reverse:</i> CCGTGTGGTTCTCCACTTTGA	PrimerBank
<i>HLA-G</i>	<i>Forward:</i> GAGGAGACACGGAACACCAAG	PrimerBank
	<i>Reverse:</i> GTCGCAGCCAATCATCCACT	PrimerBank
<i>ITGB6</i>	<i>Forward:</i> CTCAACACAATAAAGGAGCTGGG	PrimerBank
	<i>Reverse:</i> AAAGGGGATACAGGTTTTTCCAC	PrimerBank
<i>VTCN1</i>	<i>Forward:</i> TCTGGGCATCCCAAGTTGAC	PrimerBank
	<i>Reverse:</i> TCCGCCTTTTGATCTCCGATT	PrimerBank
<i>GABRP</i>	<i>Forward:</i> TTTCTCAGGCCCAATTTTGGT	PrimerBank
	<i>Reverse:</i> GCTGTCCGAGGTATATGGTGG	PrimerBank
<i>MUC16</i>	<i>Forward:</i> GGAGCACACGCTAGTTCAGAA	PrimerBank
	<i>Reverse:</i> GGTCTCTATTGAGGGGAAGGT	PrimerBank
<i>HAND1</i>	<i>Forward:</i> CCAAGGATGCACAGTCTGG	PrimerBank
	<i>Reverse:</i> AGGAGGAAAACCTTCGTGCTG	PrimerBank
<i>POSTN</i>	<i>Forward:</i> GAAAGGGAGTAAGCAAGGGAG	Dobrev <i>et al.</i> <sup>5</sup>
	<i>Reverse:</i> ATAATGTCCAGTCTCCAGGTTG	Dobrev <i>et al.</i> <sup>5</sup>
<i>TFAP2A</i>	<i>Forward:</i> GCATATCCGTTACGCCGAT	Tadeu <i>et al.</i> <sup>6</sup>
	<i>Reverse:</i> GGGAGATTGACCTACAGTGCC	Tadeu <i>et al.</i> <sup>6</sup>
<i>TFAP2B</i>	<i>Forward:</i> AGCAAATGTCACGTTACTCACC	PrimerBank
	<i>Reverse:</i> TGTGCTGCCGGTTCAAATACT	PrimerBank
<i>KRT17</i>	<i>Forward:</i> AAGATCCGTGACTGGTACCAGAGG	Sankar <i>et al.</i> <sup>7</sup>
	<i>Reverse:</i> GATGTCGGCCTCCACACTCAGG	Sankar <i>et al.</i> <sup>7</sup>
<i>KRT18</i>	<i>Forward:</i> TCGCAAATACTGTGGACAATGC	PrimerBank
	<i>Reverse:</i> GCAGTCGTGTGATATTGGTGT	PrimerBank
<i>BMP2</i>	<i>Forward:</i> ACTACCAGAAACGAGTGGGAA	PrimerBank
	<i>Reverse:</i> GCATCTGTTCTCGGAAAACCT	PrimerBank
<i>BMP4</i>	<i>Forward:</i> TCCACAGCACTGGTCTTGAG	Xu <i>et al.</i> <sup>8</sup>
	<i>Reverse:</i> GGGATGTTCTCCAGATGTTCTT	Xu <i>et al.</i> <sup>8</sup>
<i>BMP6</i>	<i>Forward:</i> AGCGACACCACAAAGAGTTCA	PrimerBank
	<i>Reverse:</i> GCTGATGCTCCTGTAAGACTTGA	PrimerBank
<i>BMP7</i>	<i>Forward:</i> TCGGCACCCATGTTTCATGC	PrimerBank
	<i>Reverse:</i> GAGGAAATGGCTATCTTGCAGG	PrimerBank

NA: not applicable.

**Supplementary Table 8. Summary of normalized gene expression fold change (Gene FC, blue) and corresponding P-values (red) in qRT-PCR results shown in Fig. 4a-e and Fig. 5c.**

Gene FC*	Glass-2D	Gel-2D	Glass-3D	Gel-3D	PS-2D	P-Value*	Gel-2D	Glass-3D	Gel-3D	PS-2D
<i>NANOG</i>	1	1.1522	0.9595	0.4603	0.0578	<i>NANOG</i>	0.0598	0.7934	0.0012	2E-05
<i>OCT4</i>	1	0.9478	1.0273	0.7412	0.3924	<i>OCT4</i>	0.6499	0.8433	0.1212	0.0008
<i>SOX2</i>	1	0.6568	0.6266	0.2098	NT	<i>SOX2</i>	0.1442	0.1137	0.0098	NT
<i>CDH1</i>	1	0.7587	0.6224	1.8445	0.464	<i>CDH1</i>	0.0735	0.0154	0.059	0.001
<i>CDH2</i>	1	0.7448	0.801	0.2637	11.195	<i>CDH2</i>	0.0622	0.1887	0.0007	5E-07
<i>CLDN6</i>	1	0.8372	1.05	1.4517	NT	<i>CLDN6</i>	0.4658	0.8044	0.1833	NT
<i>BRA</i>	1	0.5262	0.3759	18.8	1585.6	<i>BRA</i>	0.0544	0.0373	0.0006	2E-06
<i>SNAI1</i>	1	0.9643	1.1466	1.4097	7.6408	<i>SNAI1</i>	0.6599	0.1172	0.1472	2E-07
<i>SNAI2</i>	1	1	1.0984	2.5537	1.4433	<i>SNAI2</i>	0.9806	0.0914	0.0238	0.0052
<i>FOXA2</i>	1	0.6132	1.2135	0.0437	8.4235	<i>FOXA2</i>	0.5387	0.8252	0.1609	9E-05
<i>GATA2</i>	1	1.8771	2.0677	160.32	NT	<i>GATA2</i>	0.1114	0.034	0.0005	NT
<i>GATA3</i>	1	8.1577	6.3796	3040.2	NT	<i>GATA3</i>	0.0931	0.0992	0.0008	NT
<i>CDX2</i>	1	9.0195	19.566	530.69	NT	<i>CDX2</i>	0.088	0.2608	0.0011	NT
<i>TP63</i>	1	71.724	12.463	23429	NT	<i>TP63</i>	0.1116	0.0099	0.0295	NT
<i>GATA4</i>	1	0.1935	0.0778	1.7343	NT	<i>GATA4</i>	0.1331	0.093	0.2494	NT
<i>GATA6</i>	1	5.0452	0.4693	3.3463	NT	<i>GATA6</i>	0.0718	0.4822	0.2649	NT
<i>KRT7</i>	1	0.5512	0.3986	1.9239	NT	<i>KRT7</i>	0.0021	0.0004	0.3007	NT
<i>CGA</i>	1	0.4663	0.7821	3.304	NT	<i>CGA</i>	0.1149	0.6359	0.214	NT
<i>HLA-G</i>	1	0.3727	0.3892	0.4052	NT	<i>HLA-G</i>	0.0018	0.0033	0.0277	NT
<i>ITGB6</i>	1	4.7892	0.9671	591.74	NT	<i>ITGB6</i>	0.248	0.9684	0.0044	NT
<i>GABRP</i>	1	0.869	1.1178	24.297	NT	<i>GABRP</i>	0.2839	0.4897	0.0155	NT
<i>VTCN1</i>	1	0.7895	0.0355	104.82	NT	<i>VTCN1</i>	0.6431	0.0102	0.0043	NT
<i>MUC16</i>	1	0.3802	0.786	2.9286	NT	<i>MUC16</i>	0.0201	0.3676	0.0107	NT
<i>HAND1</i>	1	135.68	116.46	30774	NT	<i>HAND1</i>	0.0786	0.1017	0.0014	NT
<i>KRT17</i>	1	0.5576	0.4645	2.9104	NT	<i>KRT17</i>	0.0377	0.0256	0.001	NT
<i>KRT18</i>	1	0.9496	1.071	3.3393	NT	<i>KRT18</i>	0.7013	0.4844	0.0091	NT

<i>POSTN</i>	1	1.0868	0.8867	3.2717	<i>NT</i>	<i>POSTN</i>	0.8399	0.7694	0.012	<i>NT</i>
<i>TFAP2A</i>	1	72.791	21.807	14184	<i>NT</i>	<i>TFAP2A</i>	0.0665	0.1232	0.0023	<i>NT</i>
<i>TFAP2B</i>	<i>ND</i>	1	0.1237	111.7	<i>NT</i>	<i>TFAP2B</i>	<i>NA</i>	0.1047**	0.0097**	<i>NT</i>
<i>BMP2</i>	1	0.7732	0.4749	2.9862	<i>NT</i>	<i>BMP2</i>	0.2583	0.0147	0.0041	<i>NT</i>
<i>BMP4</i>	1	1.3545	0.8368	66.177	<i>NT</i>	<i>BMP4</i>	0.4753	0.6676	6E-06	<i>NT</i>
<i>BMP6</i>	1	0.7351	0.5598	0.1727	<i>NT</i>	<i>BMP6</i>	0.2505	0.0473	0.0029	<i>NT</i>
<i>BMP7</i>	1	1.0348	0.9192	1.7012	<i>NT</i>	<i>BMP7</i>	0.8611	0.5411	0.0132	<i>NT</i>

*ND*: not detected;

*NA*: not applicable;

*NT*: not tested;

\*: Normalized gene expression fold change and *P*-values were all calculated in comparison to the Glass-2D condition, unless noted otherwise. *P*-values were calculated using un-paired, two-sided Student's *t*-test;

\*\**P*-values were calculated in comparison to the Gel-2D condition.

**Supplementary Table 9. Summary of normalized gene expression fold change (Gene FC, blue) and corresponding P-values (red) in qRT-PCR results of the BMP inhibition assay (Supplementary Fig. 11c).**

Gene FC*	Glass-2D	Gel-3D	LDN-d2	LDN-d2&3	P-value*	Gel-3D	LDN-d2	LDN-d2&3
<i>GATA2</i>	1	172.7417	14.0872	4.3722	<i>GATA2</i>	0.0098	0.0538	0.2703
<i>GATA3</i>	1	1531.6606	90.6801	43.6863	<i>GATA3</i>	7.44E-06	7.02E-04	1.20E-03
<i>CDX2</i>	1	49.4718	7.3310	1.1481	<i>CDX2</i>	0.0281	0.2280	0.8820
<i>TP63</i>	ND	12446.1197	1497.5686	1046.1600	<i>TP63</i>	0.0067**	0.5894**	NA
<i>BMP4</i>	1	29.9719	5.8027	3.2391	<i>BMP4</i>	0.0238	0.0945	0.2471
<i>ITGB6</i>	1	723.4922	91.4117	55.6471	<i>ITGB6</i>	0.0016	0.0133	0.0772
<i>VTCN1</i>	1	105.4589	3.1638	1.7348	<i>VTCN1</i>	0.0004	0.0610	0.9567
<i>GABRP</i>	1	20.6821	1.2107	0.9584	<i>GABRP</i>	0.0302	0.3096	0.9878
<i>MUC16</i>	1	1.6520	0.7210	0.5805	<i>MUC16</i>	0.0434	0.1593	0.0495
<i>HAND1</i>	1	21838.7241	1567.4955	838.0578	<i>HAND1</i>	4.55E-06	9.40E-05	1.30E-04
<i>POSTN</i>	1	3.1656	0.9302	1.0339	<i>POSTN</i>	0.0178	0.8984	0.9944

ND: not detected;

NA: not applicable;

\*: Normalized gene expression fold change and *P*-values were all calculated in comparison to the Glass-2D condition, unless noted otherwise. *P*-values were calculated using un-paired, two-sided Student's *t*-test;

\*\**P*-values were calculated in comparison to the LDN-d2&3 condition.

## Supplementary References

1. Roost, M. S., *et al.* KeyGenes, a tool to probe tissue differentiation using a human fetal transcriptional atlas. *Stem Cell Rep.* **4**, 1112-1124 (2015).
2. Mallon, B. S., *et al.* StemCellDB: The human pluripotent stem cell database at the National Institutes of Health. *Stem Cell Res.* **10**, 57-66 (2013).
3. Wang, X. W., Spandidos, A., Wang, H. J. and Seed, B. PrimerBank: A PCR primer database for quantitative gene expression analysis, 2012 update. *Nucleic. Acids. Res.* **40**, D1144-D1149 (2012).
4. Li, Y. C., *et al.* BMP4-directed trophoblast differentiation of human embryonic stem cells is mediated through Delta Np63(+) cytotrophoblast stem cell state. *Development* **140**, 3965-3976 (2013).
5. Dobрева, M. P., *et al.* Periostin as a biomarker of the amniotic membrane. *Stem Cells Int.* **2012**, 987185 (2012).
6. Tadeu, A. M. B., *et al.* Transcriptional profiling of ectoderm specification to keratinocyte fate in human embryonic stem cells. *PLoS One* **10**, e0122493 (2015).
7. Sankar, S., *et al.* A novel role for keratin 17 in coordinating oncogenic transformation and cellular adhesion in ewing sarcoma. *Mol. Cell Biol.* **33**, 4448-4460 (2013).
8. Xu, J., *et al.* Transcriptional regulation of bone morphogenetic protein 4 by tumor necrosis factor and its relationship with age-related macular degeneration. *FASEB J.* **25**, 2221-2233 (2011).